Key Engineering Materials Vols. 326-328 (2006) pp. 487-492
online at http://www.scientific.net

Feasible Evaluation of Flow Properties and Stress State of Structural Materials Using Instrumented Indentation Tests

Ju-Young Kim[1, a], Jung-Suk Lee[1,b], Kyung-Woo Lee[1,c], Kwang-Ho Kim[2,d] and Dongil Kwon[1,e]

[1]School of Materials Science and Engineering, Seoul National University, San 56-1, Sillim-dong, Gwanak-gu, Seoul 151-742, Korea

[2]Frontics Inc., Research Institute of Advanced Materials, Seoul National University, San 56-1, Sillim-dong, Gwanak-gu, Seoul 151-742, Korea

[a]juyoung1@snu.ac.kr, [b]jslee119@snu.ac.kr, [c]case77@snu.ac.kr, [d]khkim@frontics.com, [e]dongilk@snu.ac.kr

Keywords: Instrumented indentation test, Representative stress and strain, Flow properties, Weldment, Residual stress

Abstract. Flow properties and stress state are indispensable factors for safety assessment of structural materials in operation, which were evaluated using instrumented indentation tests (IITs). Flow properties were obtained by defining representative stress and strain, and IIT results for 10 steel materials were discussed by comparing with those from uniaxial tensile tests. The indentation load-depth curve is significantly affected by the presence of residual stress, and the stress-induced load change was converted to a quantitative stress value. The stress state of a friction stir-welded joint of API X80 steel was evaluated and compared with that measured by energy-dispersive X-ray diffraction.

Introduction

Instrumented indentation test (IIT) has been extensively used to evaluate mechanical properties and stress state of structural materials in operation due to non-destructive and simple experimental procedure [1-4]. Among them, the evaluation of flow properties and residual stress are powerful since these are indispensable factor for the safety assessment [2,3]. Flow properties, primarily yield strength and tensile strength, are generally considered the most fundamental mechanical properties. These properties are degraded by use, so should be measured continuously during operation [5]. Residual stress is inevitably included in the structural materials by welding, local plastic deformation, and etc. The materials failure is strongly dependent of the stress state as well as flow properties, it is important to measure the stress state of structural materials in use non-destructively. In this study, analytic models and entire procedures were reviewed for evaluating flow properties and stress state using IIT. Flow properties of 10 steel materials were measured by IIT, which were compared with those from uniaxial tensile tests. The residual stress state of a friction stir-welded joint of API X80 steel were evaluated, which were also compared with that from energy-dispersive X-ray diffraction.

Algorithms for Evaluating Flow Properties and Stress State

Flow Property Measurement Using IIT. It is well known that the relationship of true stress σ and mean pressure P_m can be expressed as [6]

$$\sigma = \left(\frac{1}{\Psi}\right) P_m = \left(\frac{1}{\Psi}\right)\left(\frac{P}{\pi a_c^{\,2}}\right), \tag{1}$$

where Ψ is a plastic constraint factor, P is the load, and a_c is the contact radius. Most research on the indentation flow curve has used this definition of true stress. However, the plastic constraint factor has been regarded as a material-independent constant or as a function of the strain-hardening exponent. In this study, a constant value of 3.0 was used for the plastic constraint factor, as verified

by finite element analysis (FEA) of various materials [7]. On the basis of the deformation shape and strain distribution under a spherical indenter, Ahn and Kwon proposed a new definition using the tangent function [8]. The displacement along the depth axis under the indenter, u_z, can be expressed geometrically as:

$$u_z = h - (R - \sqrt{R^2 - r^2}), \tag{2}$$

where R is the indenter radius and r is a radius at any point on the depth axis. The shear strain is derived by differentiating the displacement in the depth direction. The maximum shear strain is obtained at $r = a_c$ and Ahn and Kwon obtained the true strain by using a strain proportional constant:

$$\varepsilon = \left(\frac{\alpha}{\sqrt{1 - (a_c / R)^2}} \right) \left(\frac{a_c}{R} \right) = \alpha \tan \gamma, \tag{3}$$

where α was determined as 0.14 independent of material properties by FEA for various materials [7]. This definition covers a large range of true strain. Although it also contains the contradiction that maximum strain is infinite when $a_c = R$, the experiment is generally finished by the time a_c reaches 0.6R. The tensile curves should vary according to the definitions of the true strain even when the same load–depth curve is used. Therefore, the definition of true strain should be verified by excluding the parameters within that definition. True stress and strain points are obtained by continuous IIT as explained above. These points are fitted by a constitutive equation (Hollomon equation, $\sigma = K\varepsilon^n$), and K, a material constant, and n, work-hardening exponent, are determined. Since the elastic modulus is obtained by IIT, yield strength can be measured from the intersection point between the flow curve and a line with a slope of the elastic modulus 0.2% offset from origin. The ultimate tensile strain should be same as the strain-hardening exponent by the theory of instability in tension [9], and from which the tensile strength can be determined.

Stress State Evaluation Using IIT. A surface residual stress is assumed to be in an equibiaxial tensile state ($\sigma_{res,x} = \sigma_{res,y} = \sigma_{res}$, $\sigma_{res,z} = 0$) and uniform in the near-surface region (taken as about three times the indentation depth) [10,11]. If an arbitrary indentation state (h_t, L_0) is attained in an unstressed state and if the tensile in-plane stress σ_{res} is applied to the loading state at the fixed penetration depth h_t, the indentation load L_0 will be reduced to a lower load L_T due to the decrease of surface penetration resistance. The load shift $L_T - L_0$ due to the tensile stress application becomes a clue for stress quantification. The surface-normal deviator stress σ_z^D is $-2\sigma_{res}/3$ by removing the hydrostatic stress $2\sigma_{res}/3$ from the surface residual stress σ_{res} and is added to the contact pressure [11]. $L_T - L_0$ is assumed to be the product of the selected deviator stress component and its corresponding contact area A_C^T. Thus, an equation for the equibiaxial residual stress is derived in terms of the indentation load and contact area as:

$$\sigma_{res} = 3(L_0 - L_T)/(2A_C^T). \tag{4}$$

Here A_C^T in the tensile stress state is calculated from $L_T A_C^0 / L_0$ because the contact hardness H or $L_0 / A_C^0 = L_T / A_C^T$ is independent of the elastic residual stress. In order to measure the actual contact area A_C^0 with pile-up or sink-in information from an Oliver–Pharr curve analysis [5], an empirical calibration for instrumental stiffness was performed through preliminary indentation tests on API X80 steel [3].

Since the experiments and theoretical models described above treat only equibiaxial residual stress, the magnitude of the average stress effect can be determined through the instrumented indentation technique but the directionality and magnitude of an actual biaxial stress cannot. This impedes wide application of the instrumented indentation technique to complex biaxial

stress states in actual structures. If we denote one major stress component of the biaxial residual stress as $\sigma_{res,x}$ and the other as a minor stress component $\sigma_{res,y}$, $\sigma_{res,y}$ can be expressed as $\kappa\sigma_{res,x}$ using the stress ratio κ i.e., $\sigma_{res,y}/\sigma_{res,x}$. The influence of biaxial stress on the indentation plasticity also can be analysed through a similar hydrostatic stress removal method. The deformation-sensitive deviator stress component is given as $\sigma_z^D = -(1+\kappa)\sigma_{res,x}/3$ in this case. Thus, if information on κ is given, individual principal stresses can be calculated from the instrumented indentation test using Eq. 5. Note that Eq. 5 converges to Eq. 4, when a stress state approaches to the equibiaxial state or $\kappa = 1.0$.

$$\sigma_{res,x} = 3(L_0 - L_T)/((1+\kappa)A_C^T). \quad (5)$$

Lee and Kwon showed the validity of Eq. 5 by empirical indentation tests on biaxially strained specimens [3]. Several preliminary observations on the welded joints yielded a stress ratio of about 0.33, and this value was used in subsequent biaxial stress analyses [12].

Experimental Verification on Flow Properties Measurement

10 steel materials were prepared and their surfaces were finally polished with 1 μm alumina powder. IITs were performed using AIS 3000 equipment made by Frontics Inc. with load resolution 5.6 gf and depth resolution 0.1 μm. The indenter was a WC ball of radius 250 μm, and the loading-unloading speed was 0.1 mm/min. The final maximum indentation was 150 μm and 15 partial unloadings down to 50% of maximum load at each point were performed. To verify our analysis, the true stress and strain curves were measured by tensile tests at cross-head speed of 1 mm/min for specimens with gauge length 25 mm and diameter 6 mm.

Table 1. Tensile properties obtained from tensile tests and instrumented indentation tests.

Materials	Yield strength [MPa]			Tensile strength [MPa]		
	Tensile	IIT	Error [%]	Tensile	IIT	Error (%)
P91	569.7	558.7	-1.9	772.0	807.5	4.6
S45C	372.9	336.4	-9.8	883.2	843.7	-4.5
SCM21	290.2	314.9	8.5	626.5	609.3	-2.8
SCM415	237.4	230.1	-3.1	616.3	620.7	0.7
SUJ2	306.8	270.2	-11.9	907.7	862.2	-5.0
SKD11	243.4	270.1	11.0	923.1	880.1	-4.7
SKD61	348.9	361.8	3.7	896.5	882.2	-1.6
SKS3	366.4	330.9	-9.7	781.5	810.6	3.7
API X65	451.8	522.9	15.7	610.8	630.3	3.2
API X70	592.9	550.9	-7.1	782.2	770.9	-1.4

The tensile properties obtained from tensile tests and IITs are summarized in Table 1. The error range in tensile strength obtained by IIT was within ±5% of that from tensile tests. For yield strength, the error range was within ±10% except for some materials with high error value (>±10%). The first true stress-strain points were obtained with indentation depth 10 μm, which is about 4% representative strain if contact depth is calculated ignoring elastic deflection and pile-up/sink-in. Yielding happens at strains less than 0.5% for most metallic materials. The true stress-strain points with low strain value affect fitting of the constitutive equation more than the points with high strain value since the Hollomon equation is a type of exponent function, which induces large deviation in yield strength relative to tensile strength. A possible reason for the high error in yield strength is the

presence of Lüders strain, as shown in Fig. 1(b). If the length of Lüders strain is defined as ε_L, yield strain ε_y can be estimated as

$$K\varepsilon_y^{\ n} = E(\varepsilon_y - 0.002 - \varepsilon_L). \quad (6)$$

For IIT, however, it is difficult to recognize and measure Lüders strain, and we leave this issue for future study.

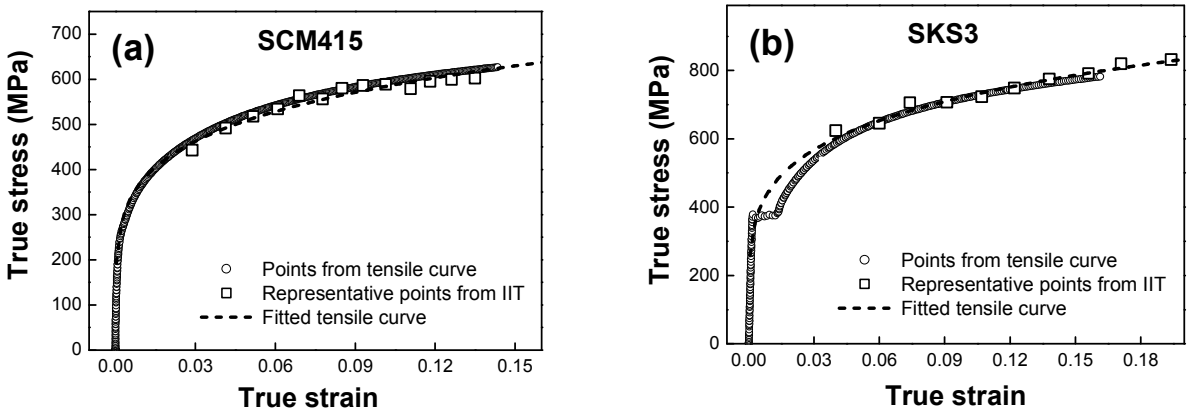

Fig. 1. Comparisons between tensile curves from uniaxial tenstile tests and instrumented indentation tests for (a) SCM415 (without Lüders strain) and (b) SKS3 (with Lüders strain).

Experimental Verification on Stress State Evalution

Experimental Procedures. API X80 steel of thickness 20 mm was used in the friction stir-welding studies; its chemical composition (wt.%) is 0.13 C, 1.52 Mn, 0.26 Si, 0.17 Mo, 0.034 Cr, 0.026 Ni, 0.0002 Nb, 0.003 Ti, 0.062 V, 0.041 Al, 0.032 Cu, 0.0003 B. Test plates were sectioned in half along the rolling direction and prepared for a butt joint. Oxide scale was removed by sand grinding followed by degreasing with methanol. An argon gas atmosphere was used to prevent oxidation during the weld cycle. Friction stir welding was done with a polycrystalline cubic boron nitride tool in an inert gas environment (MegaStir Technology, UT, USA); tool rotation and travel speeds were 550 rpm and 1.69 mms^{-1}, respectively. Metallographic samples for optical observation, Vickers microhardness, instrumented indentation test (IIT), and energy-dispersive X-ray diffraction (ED-XRD) were prepared from the welded joint using metallographic procedures followed by etching with 2% nital solution. Vickers microhardness was probed using a 0.1 kgf load across the welded joint.

A commercial AIS 3000R (Frontics, Inc., Seoul, Korea) with depth and load resolutions of 0.1 μm and 14.7 mN was used for the instrumented indentation tests, which were performed across the friction stir-welded joint at 2 mm intervals (a surface-parallel indentation testing array was made 2 mm from the welded surface). Two methods were used to obtain a reference indentation curve in a stress-free state corresponding to each microstructural region in the welds. The reference stress-free curve for the base metal, which underwent no microstructural change, was directly obtained from the remote base-metal region (about 10 mm from the welds). In addition, a multiple indentation method (5 kgf load gap) was applied to characterize contact properties at several depth steps. The reference stress-free curve for the welding zone, which underwent significant microstructural change, was calculated through a unique analysis [3]. The maximum applied load and testing speed were 50 kgf and 0.3 mm/min. We used ED-XRD with a high-energy white beam synchrotron radiation source. The profiling is done with the aid of highly collimated incident and scattered x-ray beams and with micropositioning of the sample surface. The profiling depth can attain the order of mm, and can be controlled with resolution of a few microns by radiation energy. When obtaining strain measurements using ED-XRD, we focused the depth at about 200 nm, similar to maximum indentation depth, to avoid any depth-difference effects between IIT and ED-XRD.

Residual Stress Distribution across the Friction Stir-welded Joint. The instrumented indentation curves of the BM near the HAZ (solid triangles) and the reference curve for API X80 steel are presented together in Fig. 3. The load decrease due to surface stress at a given indentation depth means that the residual stress is of positive sign (tensile). By inserting $\kappa = 0.33$ into Eq. 5, the quantitative stress distribution inside the base metal was calculated as plotted in Fig. 3. The BM reference indentation curve in Fig. 2 can be roughly fitted to $L = \alpha_B h^2$, where α_B is a hardness-proportional parameter (about upper 70% of the experimental solid line is fitted and overlapped in Fig. 2 as open triangles). The approximate reference indentation curves for the HAZ, TMAZ, and TMAZ-HZ also can be fitted by calculating corresponding α values. For example, α_{TMAZ} in the TMAZ is calculated from $\alpha_B H_{TMAX} / H_B$. The hardness ratio of the TMAZ and BM H_{TMAX} / H_B was about 1.21 and thus α_{TMAZ} was 7.76×10^9 kgf m^{-2} when α_B for the BM was given as 6.41×10^9 kgf m^{-2}. Since the remnant indent morphologies from BM and other microstructures were very similar in this study, regardless of their different indent sizes, the α value could be compared directly. If remnant indents from two materials for the α comparison have no geometrical similarity (i.e., two indents have different convexity around the contact periphery), this geometrical discrepancy must be considered in determining the α value for predicting proper shape of the loading curve.

The reference indentation curve calculated for the TMAZ-HZ is also plotted in Fig. 2 as open circles. Superposing the stressed indentation data and the newly calculated reference stress-free curve of the TMAZ, respectively, solid and open circles in Fig. 2 makes it possible to calculate a quantitative stress distribution in the TMAZ region. The stress distributions in the HAZ and TMAZ-HZ were also estimated by performing similar procedures. Finally the whole stress distribution of the friction stir-welded joint is plotted in Fig. 3 (solid circles). The residual stress profile measured from ED-XRD is also plotted in Fig. 3 (open circles). Except for the slight negative shift of the ED-XRD results (less than 50 MPa), the residual stress distributions from the IIT and ED-XRD were consistent throughout the whole welded joint. The discrepancy can be attributed to the indirectly calculated reference indentation curve and approximately determined stress ratio. The maximum tensile residual stress, about 150 MPa, was estimated near the BM-HAZ boundary, meaning that the BM-HAZ boundary is vulnerable to external loads. In addition, the high microhardness in the TMAZ-HZ region can be partially explained by the high compressive stress caused by the complex thermal cycle and phase transformation during the friction stir welding. These experimental results suggest that the instrumented indentation technique is a promising nondestructive stress-measurement technique, especially for welded joints. However, the sparse indentation results 'i.e.' the 2 mm gap preventing the deformation field overlap, should be improved for more local welds by adopting such indentation techniques as zigzag probing.

Summary

Tensile properties of 10 metallic materials were obtained using IIT by applying the representative stress and strain approach. Comparison of tensile properties from IITs with those from uniaxial tensile tests yielded an error range in the tensile strength within ±5%. For yield strength, the error range was within ±10% except for some materials with high error value (>±10%). The larger error range is basically due to the mathematical form of Hollomon equation, and the presence of Lüders strain may have affected the yield strength. The residual stress profile assessed from the instrumented indentation tests showed high tensile stress (or compressive stress) near the base metal and heat-affected zone boundary (or near the thermomechanically affected zone–hard zone). Although there was a slight difference in quantitative value, the stress trend in instrumented indentation testing was perfectly consistent with the energy-dispersive X-ray diffraction results.

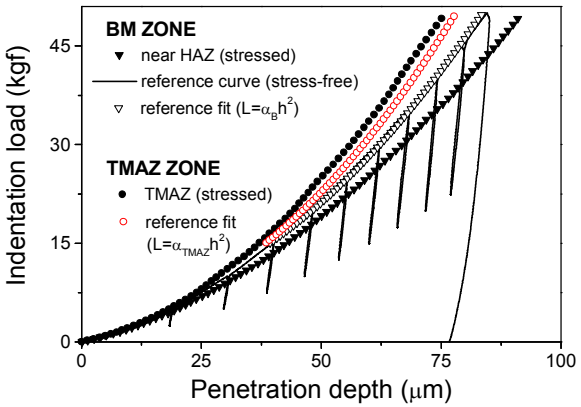

Fig. 2. Experimental indentation curves (solid triangles and circles) from the welded joint in residual stress state and analytical reference curves (open triangles and circles) in stress-free state.

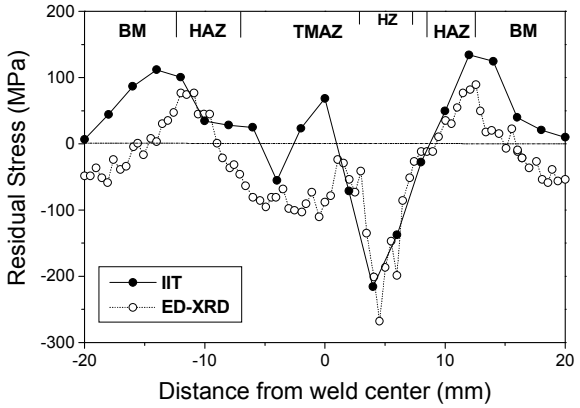

Fig. 3. Residual stress distributions measured from the instrumented indentation technique (IIT) and energy dispersive X-ray diffraction.

Acknowledgments

This research was supported partly by a grant (code #:06K1501-01111) from the *Center for Nanostructured Materials Technology* under the *21st Century Frontier R&D Program* of the Ministry of Science and Technology, Korea, and partly by a grant (code #:10023468) from the *Standardization R&D Program* of the Ministry of Commerce, Industry and Energy, Korea.

References

[1] W.C. Oliver and G.M. Pharr: J. Mater. Res. Vol. 7 (1992), p. 1564

[2] J.-Y. Kim, K.-W. Lee, J.-S. Lee and D. Kwon: Surf. Coat. Technol. (submitted for publication)

[3] Y.-H. Lee and D. Kwon: Acta Mater. Vol. 52 (2004), p. 1555

[4] J.-Y. Kim, B.-W. Lee, D.T. Read and D. Kwon: Scripta Mater. Vol. 52 (2005), p. 353

[5] J.-i. Jang, Y. Choi, Y.-H. Lee and D. Kwon: Mater. Sci. Eng. A Vol. 395 (2005), p.295

[6] D. Tabor: *Hardness of Metals* (Clarendon Press, UK 1951)

[7] E.-c. Jeon, M.-K. Baik, S.-H. Kim, B.-W. Lee and D. Kwon: Key Eng. Mater. Vol. 297-300 (2005), p. 2152

[8] J.-H. Ahn and D, Kwon: J. Mater. Res. Vol. 16 (2001), p. 3170

[9] G.E. Dieter: *Mechanical Metallurgy* (McGraw Hill, USA 1986)

[10] S. Suresh and A.E. Giannakopoulos: Acta Mater. Vol. 46 (1998), p. 5755

[11] Y.-H. Lee and D. Kwon: Scripta Mater. Vol. 49 (2003), p. 459

[12] Y. Choi, Y.-H. Lee, J.-i. Jang, S.-K. Park, K.-H. Kim, Y.-W. Seo and D. Kwon: Key Eng. Mater. Vol. 297-300 (2005), p. 2122